Volumetric formulation of the lattice Boltzmann method for fluid dynamics: Basic concept

Hudong Chen
Exa Corporation, 125 Cambridge Park Drive, Cambridge, Massachusetts 02140
(Received 25 March 1998)

A lattice Boltzmann algorithm based on a volumetric representation is formulated for achieving properties consistent with the standard form at finer resolution. In contrast to pointwise interpolation schemes, this approach can be applied to arbitrary meshes without compromising exact conservation or equilibrium properties. [S1063-651X(98)01709-7]

PACS number(s): 02.70.−c, 47.27.−i, 51.10.+y

I. INTRODUCTION

The importance of the lattice Boltzmann (LB) method for computational fluid dynamics (CFD) has recently become well recognized [1–8]. This method possesses certain clear advantages over conventional CFD methods, such as its ease in handling flows with multiple immiscible phases [9–12], and the physical implementation of complex boundary conditions. One recent effort is to extend its order of accuracy and flexibility so that its spatial resolution requirements for various flow situations may be reduced and may be adapted to more general meshes. Attempts at this have already been made based on the technique of pointwise interpolation [13]. However, such a pointwise representation, as we will realize below, has shown difficulties in preserving certain fundamental properties in LB on nonuniform meshes. In this paper we present an alternative approach based on a volumetric representation, which removes these essential difficulties. The concept of using a finite-volume approach in LB was introduced by Benzi *et al.* in 1992 [14]. However, our formulation is somewhat different and is worked out systematically in detail. Furthermore, it perhaps offers a clearer interpretation of the underlying physics. The general algorithm of the present approach is simple and is applicable with explicitly defined accuracy to arbitrary meshes. In addition, when used on uniform meshes, the resulting finite-volume Boltzmann equation is shown to produce the same hydrodynamics at lower required resolution compared to that of the standard lattice Boltzmann equation. Physically, the present formulation implies a possibility of alternative theoretical constructions of subgrid fluid turbulence models based on a Boltzmann representation rather than the Navier-Stokes hydrodynamics.

A basic LB system is conventionally represented by the Boltzmann difference equation [lattice Boltzmann equation (LBE)] on a D-dimensional Bravis lattice $\mathcal{L}_f$

$$n_i(\mathbf{x},t+\Delta t)=n_i'(\mathbf{x}-\hat{\mathbf{c}}_i,t) \quad \forall \ \mathbf{x}\in\mathcal{L}_f, \tag{1}$$

where $n_i(\mathbf{x},t)$ $(\geqslant 0)$ is the particle distribution function for momentum state $\hat{\mathbf{c}}_i$ on a lattice site $\mathbf{x}$ at time step t. The spatial vectors of the set $\{\hat{\mathbf{c}}_i; i=0,\ldots,b\}$ are links between a site to its specified neighboring sites. Physically, Eq. (1) can be interpreted as particles with momentum $\hat{\mathbf{c}}_i$ hop from lattice site $\mathbf{x}-\hat{\mathbf{c}}_i$ to its indicated destination site $\mathbf{x}$ during a time increment Δt. The quantity $n_i'(\mathbf{x},t)$ $[\equiv n_i(\mathbf{x},t)+\Omega_i(\mathbf{x},t)]$ represents a postcollision particle distribution. The difference between the pre- and the postcollision distributions $\Omega_i(\mathbf{x},t)$ is usually interpreted to be due to a collision process. It drives the system to a local equilibrium and satisfies some basic local conservation conditions

$$\sum_i \xi_i\Omega_i(\mathbf{x},t)=0, \tag{2}$$

with $\xi_i=1$, $\hat{\mathbf{c}}_i$, and possibly ϵ_i $(\equiv\hat{c}_i^2/2)$, corresponding to mass, momentum, and energy conservation, respectively. One of the simplest forms of Ω_i is the Bhatnagar-Gross-Krood (BGK) operator [7,16],

$$\Omega_i(\mathbf{x},t)=-\frac{\Delta t}{\tau}[n_i(\mathbf{x},t)-n_i^{eq}(\mathbf{x},t)], \tag{3}$$

where $n_i^{eq}(\mathbf{x},t)$ is the prescribed local equilibrium distribution function which, as indicated by Eq. (2), has the same corresponding mass, momentum and energy values as $n_i(\mathbf{x},t)$, that is,

$$\begin{aligned}
&\sum_i n_i^{eq}(\mathbf{x},t)=\sum_i n_i(\mathbf{x},t)\equiv n(\mathbf{x},t),\\
&\frac{1}{\Delta t}\sum_i \hat{c}_i n_i^{eq}(\mathbf{x},t)=\frac{1}{\Delta t}\sum_i \hat{c}_i n_i(\mathbf{x},t)\\
&\qquad\qquad\equiv n(\mathbf{x},t)\mathbf{u}(\mathbf{x},t),\\
&\frac{1}{\Delta t^2}\sum_i \epsilon_i n_i^{eq}(\mathbf{x},t)=\frac{1}{\Delta t^2}\sum_i \epsilon_i n_i(\mathbf{x},t)\\
&\qquad\qquad\equiv\frac{1}{2}n(\mathbf{x},t)\mathbf{u}^2(\mathbf{x},t)+n(\mathbf{x},t)\frac{DT(\mathbf{x},t)}{2},
\end{aligned} \tag{4}$$

where the hydrodynamic quantities $n(\mathbf{x},t)$, $\mathbf{u}(\mathbf{x},t)$ and $T(\mathbf{x},t)$ are, respectively, the site-wise particle number, fluid velocity, and temperature, respectively. According to the above, a LB dynamic system involves two fundamental steps: advection and collision. Each fundamental step satisfies the required global conservation laws exactly. It has been shown that, with some appropriate choice of lattices (such as two-dimensional hexagonal or four-dimensional face-centered-

hypercube lattices) together with suitable equilibrium forms for $n_i^{eq}(\mathbf{x},t)$ as a function of local hydrodynamic variables of $n(\mathbf{x},t)$, $\mathbf{u}(\mathbf{x},t)$, and $T(\mathbf{x},t)$, the evolutions of the hydrodynamic quantities governed by such a LB system obey the viscous Navier-Stokes fluid equations at the long-wavelength and low-frequency limit [2,7,8].

As have been pointed out by Cao *et al.* [17], the LBE represented by Eq. (1) can be viewed as just a particular first-order finite difference (on a particular mesh spanned by $\{\hat{\mathbf{c}}_i\}$) approximation to a differential equation in a continuum space

$$\frac{\partial n_i(\mathbf{x},t)}{\partial t}\Delta t+\hat{\mathbf{c}}_i\cdot\nabla n_i(\mathbf{x},t)=\Omega_i(\mathbf{x},t). \tag{5}$$

The reason that Eq. (1) is able to achieve a correct viscous hydrodynamics is that the resulting second-order spatial error term has the same form as that produced via the physical collision process, so that it can be absorbed to form a new viscosity definition. This makes the overall method on a uniform mesh second-order accurate as necessary for viscous hydrodynamics. However, such a redefined viscosity is sensitively dependent on the grid resolution and immediately breaks down when a general mesh is used. Also, because of this reason and some stability considerations, the minimum attainable viscosity value at a given resolution is still larger than desirable for the purpose of efficiently simulating high Reynolds number flows. On the other hand, the differential form of Eq. (5) is in principle not constrained by these limitations.

Nevertheless, it is convenient to keep using the LBE form of Eq. (1) as our basic starting point. We can construct another difference equation on a coarser mesh based on this discrete system defined on a denser underlying lattice. In so doing, we must make sure that the new system on a coarser mesh recovers the original finer mesh LBE with necessary accuracy for realizing the same viscous hydrodynamics.

II. POINTWISE INTERPOLATION AND ITS PROBLEMS

The most direct way to extend Eq. (1) onto a more general mesh is via a pointwise interpolation procedure [13]. Obviously, if the new mesh $\mathcal{L}_c$ is not the original lattice spanned by the basis momentum vectors $\{\hat{\mathbf{c}}_i\}$, and if $\mathbf{x}$ is a node of the new mesh, $\mathbf{x}-\hat{\mathbf{c}}_i$ may not always be another node. Hence the quantity $n_i'(\mathbf{x}-\hat{\mathbf{c}}_i,t)$ needs to be reconstructed according to the valid information on the new neighborhood mesh nodes.

To achieve necessary three-dimensional (3D) viscous hydrodynamics, it can be shown that $n_i'(\mathbf{x}-\hat{\mathbf{c}}_i,t)$ must be approximated through at least a second-order interpolation scheme. In particular, its explicit form on a 3D nonuniform Cartesian mesh can be shown to be

$$\begin{aligned} n_i'(\mathbf{x}-\hat{\mathbf{c}}_i,t)&\approx\tilde{n}_i'(\mathbf{x}-\hat{\mathbf{c}}_i,t)\\ &\equiv\sum_{\alpha=0}^{2}\sum_{\beta=0}^{2}\sum_{\gamma=0}^{2}P^i_{\alpha\beta\gamma}(\mathbf{x})\\ &\quad\times n_i'(\mathbf{x}-\boldsymbol{\Delta}^i_{\alpha\beta\gamma}(\mathbf{x}),t). \end{aligned} \tag{6}$$

In the above, $n_i'(\mathbf{x}-\boldsymbol{\Delta}^i_{\alpha\beta\gamma}(\mathbf{x}),t)$ is the postcollision distribution on a valid neighborhood node $\mathbf{x}-\boldsymbol{\Delta}^i_{\alpha\beta\gamma}(\mathbf{x})$ $(\in\mathcal{L}_c)$. Naturally, the optimal choice for obtaining the best local accuracy is for $\mathbf{x}-\boldsymbol{\Delta}^i_{\alpha\beta\gamma}(\mathbf{x})$ to be one of the nearest-neighbor nodes of $\mathbf{x}-\hat{\mathbf{c}}_i$. The geometric weight $P^i_{\alpha\beta\gamma}(\mathbf{x})$ for the second-order interpolation scheme has the form

$$\begin{aligned} P^i_{\alpha\beta\gamma}(\mathbf{x})=\prod_{\sigma=x,y,z}&\left(\frac{\Delta^i_{\alpha'\beta'\gamma',\sigma}(\mathbf{x})-c_{i,\sigma}}{\Delta^i_{\alpha'\beta'\gamma',\sigma}(\mathbf{x})-\Delta^i_{\alpha\beta\gamma,\sigma}(\mathbf{x})}\right)\\ &\times\left(\frac{\Delta^i_{\alpha''\beta''\gamma'',\sigma}(\mathbf{x})-c_{i,\sigma}}{\Delta^i_{\alpha''\beta''\gamma'',\sigma}(\mathbf{x})-\Delta^i_{\alpha\beta\gamma,\sigma}(\mathbf{x})}\right) \end{aligned} \tag{7}$$

where the subscript $\alpha'=\alpha+1(\mathrm{mod}2)$ and $\alpha''=\alpha+2(\mathrm{mod}2)$. Similar definitions apply to β', β'', γ', and γ''. It is readily verified that

$$\sum_{\alpha=0}^{2}\sum_{\beta=0}^{2}\sum_{\gamma=0}^{2}P^i_{\alpha\beta\gamma}(\mathbf{x})=1\quad\forall\ \mathbf{x}\in\mathcal{L}_c, \tag{8}$$

which is the detailed-balance relation necessary to admit the physical uniform flow as an equilibrium solution of the system. On the other hand, one can see that the global particle conservation via advection requires the normalizability condition

$$\sum_{\alpha=0}^{2}\sum_{\beta=0}^{2}\sum_{\gamma=0}^{2}P^i_{\alpha\beta\gamma}(\mathbf{x}+\boldsymbol{\Delta}^i_{\alpha\beta\gamma}(\mathbf{x}))=1\quad\forall\ \mathbf{x}\in\mathcal{L}_c. \tag{9}$$

Thus if the condition is realized, one can show that summation over all nodes in the system gives

$$\sum_{\mathbf{x}}\tilde{n}_i'(\mathbf{x}-\hat{c}_i,t)=\sum_{\mathbf{x}}n_i'(\mathbf{x},t) \tag{10}$$

when boundary conditions are ignored.

Several features of such a scheme are worth noting. First of all, it is straightforward to show that the second-order interpolation $\tilde{n}_i'(\mathbf{x}-\hat{\mathbf{c}}_i,t)$ gives the same result up to the second-order spatial derivatives as $n_i'(\mathbf{x}-\hat{\mathbf{c}}_i,t)$. Therefore, it gives rise to the same hydrodynamics having the same leading order viscous transport coefficient values as that of the LBE. Second, if the new mesh is a uniform one, then, as in the original LBE, the global particle conservation is satisfied exactly by the second-order approximation. This is because $P^i_{\alpha\beta\gamma}(\mathbf{x})$ for uniform meshes becomes independent of $\mathbf{x}$, so that the normalizability condition (9) and the detailed-balance relation (8) are satisfied simultaneously. As a particular example, we select the neighboring Cartesian mesh nodes of $\mathbf{x}-\hat{\mathbf{c}}_i$ to be $\{\mathbf{x}-\boldsymbol{\Delta}^i_{\alpha\beta\gamma};\alpha,\beta,\gamma=0,1,2\}$, with

$$\begin{aligned} \boldsymbol{\Delta}^i_{\alpha\beta\gamma}=&\,\mathrm{sgn}(c_{i,x})\alpha\Delta_x\hat{x}+\mathrm{sgn}(c_{i,y})\beta\Delta_y\hat{y}\\ &+\mathrm{sgn}(c_{i,z})\gamma\Delta_z\hat{\mathbf{z}}, \end{aligned} \tag{11}$$

where $\hat{\mathbf{x}}$, $\hat{\mathbf{y}}$, and $\hat{\mathbf{z}}$ are the unit vectors indicating the three Cartesian coordinate directions. Δ_σ $(\sigma=x,y,\text{or }z)$ represents the distance between two nearest-neighbor nodes along the x, y, or z direction, respectively. For this case, the weight takes a simple form

$$P^i_{\alpha\beta\gamma}=P^{i,x}_\alpha P^{i,y}_\beta P^{i,z}_\gamma, \tag{12}$$

with

$$\begin{aligned} P_0^{i,\sigma}&=\left(\frac{\Delta_\sigma-|c_{i,\sigma}|}{\Delta_\sigma}\right)\left(\frac{2\Delta_\sigma-|c_{i,\sigma}|}{2\Delta_\sigma}\right),\\ P_1^{i,\sigma}&=\left(\frac{|c_{i,\sigma}|}{\Delta_\sigma}\right)\left(\frac{2\Delta_\sigma-|c_{i,\sigma}|}{\Delta_\sigma}\right),\\ P_2^{i,\sigma}&=-\left(\frac{|c_{i,\sigma}|}{2\Delta_\sigma}\right)\left(\frac{\Delta_\sigma-|c_{i,\sigma}|}{\Delta_\sigma}\right). \end{aligned} \tag{13}$$

Based on physical considerations [2,8], we know that exact conservation laws are essential for such a system to realize a fully self-consistent and stable microdynamics at all times, even though the method is only second-order accurate in achieving Navier-Stokes hydrodynamics. Unfortunately, such exact conservation conditions are lost in the above second-order pointwise interpolation scheme for nonuniform meshes. In fact, the conservation laws themselves also become only second-order accurate. One might attempt to modify the geometric weights in order to reenforce the exact conservations. The problem is that in so doing it does not seem possible to avoid violating the detailed balance relations necessary for maintaining absolute equilibrium, so that local anomalous currents or gradients emerge out of a quiescent unforced situation. Moreover, there are additional minor undesirable features in such a scheme. For instance, the number of neighborhood points used for interpolating a 3D point is relatively large ($=27$) for performing efficient computations. Another physically undesirable problem is that at least one of the weights, $P^i_{\alpha\beta\gamma}$ is negative. This means that a negative amount of particles propagate in several directions. Consequently, negative particle distributions may occur at some local spatial domains under certain circumstances.

III. VOLUMETRIC FORMULATION ON A GENERAL MESH

The key problem associated with the pointwise representation is that the density function is not well defined due to the lack of a volumetric measure, except for the trivial uniform mesh situation in which the sitewise particle number $n(\mathbf{x},t)$ can be interpreted as the number density.

An alternative formalism is to adopt the finite-volume concept [14,15]. Instead of viewing particles as residing on discrete mesh nodes, we imagine a continuum space being divided into cells of various shapes and volumes. We can label a cell by the mesh node $\overline{\mathbf{x}}$ it encloses. The volume of the cell $\overline{\mathbf{x}}$ is given by

$$V(\overline{\mathbf{x}})\equiv\int_{D(\overline{\mathbf{x}})} d^3x, \tag{14}$$

where the volume integration is restricted in the spatial domain $D(\overline{\mathbf{x}})$ defined for the cell. The summation of all cell domains should be equal to the entire continuum spatial space $\mathcal{M}$ of the system; otherwise there is no unique choice of each cell domain. On the other hand, it is advantageous and convenient to construct them in such a way that (i) it naturally reduces to cells of equal shape and volume for the cases of uniform meshes and (ii) the mesh node coincides with the geometric center of its corresponding cell defined as

$$\overline{\mathbf{x}}=\frac{1}{V(\overline{\mathbf{x}})}\int_{D(\overline{\mathbf{x}})}\mathbf{x}\, d^3x. \tag{15}$$

Because we have now a well-defined volumetric measure given by Eq. (14), the mean distribution function density for cell $\overline{\mathbf{x}}$ can be defined as

$$n_i(\overline{\mathbf{x}},t)\equiv N_i(\overline{\mathbf{x}},t)/V(\overline{\mathbf{x}}),\quad \overline{\mathbf{x}}\in\mathcal{L}_c, \tag{16}$$

where $N_i(\overline{\mathbf{x}})$ is the total particle number with momentum $\hat{\mathbf{c}}_i$ residing within cell $\overline{\mathbf{x}}$.

We imagine that the space spanned on the original denser lattice grids by $\{\hat{\mathbf{c}}_i\}$ is now divided into various subspaces specified by the cell domains and particles have a continuous distribution within each cell domain. If the particles advect according to the original lattice velocities, then some portion of the particles in a cell will move across the cell boundary into other cells. This is a coarse-grained representation of the original underlying lattice dynamics in the finite-volume sense. Note the coarse-grained representation is not an approximation if the exact particle distributions within a cell are known. The finite-volume lattice Boltzmann equation can be described by the generic expression

$$N_i(\overline{\mathbf{x}},t+\Delta t)=\sum_{\overline{\mathbf{x}}'} F_i(\overline{\mathbf{x}}'\to\overline{\mathbf{x}},t), \tag{17}$$

where $N_i(\overline{\mathbf{x}},t+\Delta t)$ is the total particle number with momentum $\hat{\mathbf{c}}_i$ in cell $\overline{\mathbf{x}}$ at time step $t+\Delta t$. $F_i(\overline{\mathbf{x}}'\to\overline{\mathbf{x}},t)$, referred to as the state-flux function, represents the number of particles with momentum $\hat{\mathbf{c}}_i$ that cross from cell $\overline{\mathbf{x}}'$ to $\overline{\mathbf{x}}$ during time t to $t+\Delta t$ due to advection. Global particle conservation is guaranteed if the state-flux function satisfies the condition

$$\sum_{\overline{\mathbf{x}}} F_i(\overline{\mathbf{x}}'\to\overline{\mathbf{x}},t)=N_i'(\overline{\mathbf{x}}',t)\quad \forall\ \overline{\mathbf{x}}'\in\mathcal{L}_c. \tag{18}$$

It is easily recognized that the finite-volume representation gives the same results if the state-flux function exactly corresponds to the original particle dynamics on the underlying lattice. Specifically, the sufficient condition for achieving the original LBE is

$$\sum_{\overline{\mathbf{x}}'} F_i(\overline{\mathbf{x}}'\to\overline{\mathbf{x}},t)=V(\overline{\mathbf{x}})n_i'(\overline{\mathbf{x}}-\hat{\mathbf{c}}_i,t), \tag{19}$$

where $n_i'(\overline{\mathbf{x}}-\hat{c}_i,t)$ is the postcollision state density function at $\overline{\mathbf{x}}-\hat{c}_i$ ($\in\mathcal{L}_f$). The proof is trivial by plugging Eq. (19) into Eq. (17) directly. However, to realize up to the correct viscous order hydrodynamics, it can be shown that we require only

$$\sum_{\overline{\mathbf{x}}'} F_i(\overline{\mathbf{x}}'\rightarrow\overline{\mathbf{x}},t)=V(\overline{\mathbf{x}})[1-\hat{\mathbf{c}}_i\cdot\boldsymbol{\nabla}+\tfrac{1}{2}\hat{\mathbf{c}}_i\hat{\mathbf{c}}_i:\boldsymbol{\nabla}\boldsymbol{\nabla}]\times n_i'(\overline{\mathbf{x}},t)+O(\boldsymbol{\nabla}^3), \tag{20}$$

which is an approximation to Eq. (19) by keeping Taylor expanded terms to the second order.

We need to construct the above state-flux function $F_i(\overline{\mathbf{x}}'\rightarrow\overline{\mathbf{x}},t)$ based only on information that exists on the new mesh nodes. We first introduce the notion of a density distribution $\tilde{n}_i(\mathbf{x},t)$ inside each continuous cell domain space $\mathbf{x}\in D(\overline{\mathbf{x}})$. Hence

$$\int_{D(\overline{\mathbf{x}})}\tilde{n}_i(\mathbf{x},t)d^3x=N_i'(\overline{\mathbf{x}},t)\equiv V(\overline{\mathbf{x}})n_i'(\overline{\mathbf{x}},t) \tag{21}$$

where $N_i'(\overline{\mathbf{x}},t)$ is the postcollision particle number with momentum $\hat{\mathbf{c}}_i$ in cell $\mathbf{x}$. Using this notion, the state-flux function can be immediately constructed: Advection by $\hat{\mathbf{c}}_i$ simply performs a rigid-body translation of the distribution from its original spatial domain [i.e., $D(\overline{\mathbf{x}})$] to a new domain. As a result, the fraction of particles in the original cell $\overline{\mathbf{x}}$ that will fall into a new cell $\overline{\mathbf{x}}'$ are the particles initially residing in a subdomain of $D(\overline{\mathbf{x}})$ that overlaps with $D^{-i}(\overline{\mathbf{x}}')$. The latter represents a domain of space that is a rigid-body translation of $D(\overline{\mathbf{x}}')$ by $-\hat{\mathbf{c}}_i$. Based on this picture, we can readily express the state-flux function as

$$F_i(\overline{\mathbf{x}}\rightarrow\overline{\mathbf{x}}',t)=\int_{D(\overline{\mathbf{x}})\cap D^{-i}(\overline{\mathbf{x}}')}\tilde{n}_i(\mathbf{x},t)d^3x. \tag{22}$$

Apparently, the finite-volume representation produces equivalent dynamics if $\tilde{n}_i(\mathbf{x},t)$ were to correspond to the particle distribution on the original underlying lattice.

Theorem. A sufficient condition for achieving Eq. (20) is to have

$$\tilde{n}_i(\mathbf{x},t)=n_i'(\overline{\mathbf{x}},t)+(\mathbf{x}-\overline{\mathbf{x}})\cdot\tilde{\boldsymbol{\nabla}}n_{i'}(\overline{\mathbf{x}},t)+\tfrac{1}{2}(\mathbf{x}-\overline{\mathbf{x}})(\mathbf{x}-\overline{\mathbf{x}}):\tilde{\boldsymbol{\nabla}}\tilde{\boldsymbol{\nabla}}n_i'(\overline{\mathbf{x}},t), \tag{23}$$

where $\tilde{\boldsymbol{\nabla}}$ and $\tilde{\boldsymbol{\nabla}}\tilde{\boldsymbol{\nabla}}$ represent finite-difference approximations based on $\mathcal{L}_c$ to the spatial gradient $\boldsymbol{\nabla}$ and $\boldsymbol{\nabla}\boldsymbol{\nabla}$, respectively, which must be accurate up to $O(\nabla^2)$.

A detailed proof is given in the Appendix. Here we provide explanations of some essential features. The explicit form in Eq. (23) suggests that it is not enough to simply treat the distribution as constant inside each cell, which would be the case if the second and third terms were neglected. Indeed, when there are differences in particle densities among cells in the vicinity, continuity suggests that the distribution within a cell domain would not be a constant if a finer grid were present. As one can see directly (cf. the Appendix), these additional gradient terms $\boldsymbol{\nabla}n_i'(\overline{\mathbf{x}},t)$ and $\boldsymbol{\nabla}\boldsymbol{\nabla}n_i'(\overline{\mathbf{x}},t)$ are necessary to produce correct convection and diffusion hydrodynamic properties for an arbitrary mesh. Therefore, we should reconstruct them based on the available neighborhood information. The corresponding state-flux function given by Eqs. (22) and (23) can be integrated to give

$$F_i(\overline{\mathbf{x}}\rightarrow\overline{\mathbf{x}}',t)=V_i(\overline{\mathbf{x}},\overline{\mathbf{x}}')[n_i'(\overline{\mathbf{x}},t)+\mathbf{A}_i(\overline{\mathbf{x}},\overline{\mathbf{x}}')\cdot\tilde{\boldsymbol{\nabla}}n_i'(\overline{\mathbf{x}},t)+\mathbf{B}_i(\overline{\mathbf{x}},\overline{\mathbf{x}}'):\tilde{\boldsymbol{\nabla}}\tilde{\boldsymbol{\nabla}}n_i'(\overline{\mathbf{x}},t)] \tag{24}$$

where the purely geometric quantities $V_i(\overline{\mathbf{x}},\overline{\mathbf{x}}')$, $\mathbf{A}_i(\overline{\mathbf{x}},\overline{\mathbf{x}}')$ and $\mathbf{B}_i(\overline{\mathbf{x}},\overline{\mathbf{x}}')$ are completely determined once the mesh and all the associated cell shapes are specified. These are

$$V_i(\overline{\mathbf{x}},\overline{\mathbf{x}}')\equiv\int_{D(\overline{\mathbf{x}})\cap D^{-i}(\overline{\mathbf{x}}')}d^3x,$$

$$V_i(\overline{\mathbf{x}},\overline{\mathbf{x}}')\mathbf{A}_i(\overline{\mathbf{x}},\overline{\mathbf{x}}')\equiv\int_{D(\overline{\mathbf{x}})\cap D^{-i}(\overline{\mathbf{x}}')}(\mathbf{x}-\overline{\mathbf{x}})d^3x, \tag{25}$$

$$V_i(\overline{\mathbf{x}},\overline{\mathbf{x}}')\mathbf{B}_i(\overline{\mathbf{x}},\overline{\mathbf{x}}')\equiv\int_{D(\overline{\mathbf{x}})\cap D^{-i}(\overline{\mathbf{x}}')}\frac{1}{2}(\mathbf{x}-\overline{\mathbf{x}})(\mathbf{x}-\overline{\mathbf{x}})d^3x.$$

In particular, if a Cartesian (not necessarily uniform) mesh is used, these geometric quantities, as well as the finite differences of the derivatives, can be analytically expressed because of the simple rectangular cell shapes and integration boundaries. However, due to their tedious mathematical expressions, we omit presenting them here. The physical meaning of Eq. (24) is clear: The quantity $V_i(\overline{\mathbf{x}},\overline{\mathbf{x}}')$ is simply the overlapping volume between two cells due to advection. If we had assumed the particle distribution inside a cell to be uniform, then the number of particles that move from one cell to another would just be $V_i(\overline{\mathbf{x}},\overline{\mathbf{x}}')N_i'(\overline{\mathbf{x}},t)/V(\overline{\mathbf{x}})$, which trivially adds up to give the total particle number defined by Eq. (21). However, the additional terms in Eq. (23) do not in general satisfy Eq. (21). [We can recognize that this is because of the second derivative term in Eq. (23).] This does not pose a problem with regard to exact particle conservation in the system since it is determined by the condition for the state-flux function (18). For such a purpose, we can simply redefine the ''self-advection'' part of state-flux function by including an extra term

$$F_i(\overline{\mathbf{x}}\rightarrow\overline{\mathbf{x}},t)=N_i'(\overline{\mathbf{x}},t)-\sum_{\overline{\mathbf{x}}'\neq\overline{\mathbf{x}}}F_i(\overline{\mathbf{x}}\rightarrow\overline{\mathbf{x}}',t)\equiv\int_{D(\overline{\mathbf{x}})\cap D^{-i}(\overline{\mathbf{x}}')}\tilde{n}_i(\mathbf{x},t)d^3x+\theta_i(\overline{\mathbf{x}},t), \tag{26}$$

where the other state-flux functions (for $\overline{\mathbf{x}}'\neq\overline{\mathbf{x}}$) are still defined by Eqs. (22) and (23). Fortunately (shown in the Appendix), the extra term in Eq. (26) does not introduce any error in the resulting hydrodynamics. Consequently, the particle conservation laws are exactly enforced.

Unlike the pointwise interpolation scheme, it is important to realize that the equilibrium condition is also automatically satisfied by Eqs. (24) and (26). This is because when the fluid is spatially homogeneous $[n_i'(\overline{\mathbf{x}},t)=n_i(\overline{\mathbf{x}},t)=\overline{n}_i]$, the gradient terms vanish [and so does $\theta_i(\overline{\mathbf{x}},t)$ in Eq. (26)]. Plugging it in Eq. (17) we have

$$V(\overline{\mathbf{x}})n_i=\sum_{\overline{\mathbf{x}}'} V_i(\overline{\mathbf{x}}',\overline{\mathbf{x}})n_i. \tag{27}$$

Hence the constant density distribution is an equilibrium solution of the dynamic equation if

$$\sum_{\overline{\mathbf{x}}'} V_i(\overline{\mathbf{x}}',\overline{\mathbf{x}})=V(\overline{\mathbf{x}}). \tag{28}$$

This is indeed the case due to the volumetric measure defined above. Note, as mentioned previously, that this property is not automatically satisfied in the pointwise interpolation scheme. Equation (17), together with Eqs. (24) and (26), completely specifies the finite-volume coarse-grained lattice Boltzmann algorithm on any general mesh.

IV. SUPERGRID LATTICE DYNAMICS

The above basic formalism is valid for any choice of mesh. However, it is in fact quite useful to apply the present method even to a uniform Cartesian mesh. In particular, we can choose the mesh $\mathcal{L}_c$ to be the same lattice as for the original LBE but with coarser resolution, so that each new cell now becomes a block containing an integer multiple of original cells. If we define Δ and c as the linear dimensions of the coarser and the original cells, respectively, then each new cell contains $M=(\Delta/c)^D$ original cells. As discussed previously, the standard LBE produces higher than desirable viscous effects at a given lattice resolution. In contrast, the present formulation is essentially a higher-order numerical scheme: It produces the same viscous hydrodynamics in the long-wavelength limit with a coarser resolution as the standard LBE. The physical reason why the present system is capable of accomplishing this is the fact that the particle distribution within a cell has virtually a nonuniform profile, while it is simply a constant for the original LBE. Another reason is related to having a more relaxed Courant condition in the formulation. Compared to the pointwise interpolation scheme, the present volumetric scheme is more efficient as a numerical algorithm and also possesses much clearer physical meaning as a self-consistent dynamical system. Physically, the present formalism can be interpreted as a ''block spin'' representation of the original finer mesh LB system. It has been generally argued that a coarse-graining realization of an underlying continuum (or fine grained) process is more accurate than that of the conventional finite differencing [18].

For the particular case of a uniform Cartesian mesh, the formulation presented here becomes significantly simplified. The specific reason for the significant simplification is that, because of some self-cancellations, the second derivative terms in Eqs. (23) and (24) can be omitted without sacrificing accuracy in the resulting hydrodynamics. This feature can be verified directly by showing that the expression (24) without the second-derivative term still gives rise to Eq. (20) on a uniform mesh. Also, because of the exclusion of the second-derivative terms, Eq. (21) now becomes exactly satisfied. All the geometric quantities defined above for a uniform Cartesian mesh can be easily calculated analytically. For example, the cell volume is just $V(\mathbf{x})=V=\Delta_x\Delta_y\Delta_z$, where Δ_σ $(\sigma=x,y,z)$ is the distance between two nearest-neighbor mesh nodes along the σ Cartesian coordinate direction.

After straightforward volumetric integrations, we arrive at the algorithm for the finite-volume supergrid lattice Boltzmann equation on a uniform Cartesian mesh

$$N_i(\mathbf{x},t+\Delta t)=\sum_{\alpha=0}^{1}\sum_{\beta=0}^{1}\sum_{\gamma=0}^{1} F_i(\mathbf{x}-\boldsymbol{\Delta}^i_{\alpha\beta\gamma}\rightarrow\mathbf{x},t), \tag{29}$$

where $\boldsymbol{\Delta}^i_{\alpha\beta\gamma}$ has the same form as Eq. (11), but its subindices only go up to 1. The state-flux function has the explicit form

$$F_i(\mathbf{x}\rightarrow\mathbf{x}+\boldsymbol{\Delta}^i_{\alpha\beta\gamma},t)=P^{i,x}_\alpha P^{i,y}_\beta P^{i,z}_\gamma[N'_i(\mathbf{x},t)+\delta N'_{i,\alpha\beta\gamma}(\mathbf{x},t)], \tag{30}$$

where the weights have the simple forms, the same as for an linear interpolation,

$$P^{i,\sigma}_0=1-\frac{|c_{i,\sigma}|}{\Delta_\sigma},\qquad P^{i,\sigma}_1=\frac{|c_{i,\sigma}|}{\Delta_\sigma}, \tag{31}$$

which are positive for the choice of $\Delta_\sigma\geqslant\max(|c_{i,\sigma}|;i=1,\ldots,b)$ and $\sigma=x,y,z$. The quantity $\delta N'_{i,\alpha\beta\gamma}(\mathbf{x},t)$, which is caused by a virtual spatial inhomogeneity within a cell, is defined as

$$\begin{aligned}\delta N'_{i,\alpha\beta\gamma}(\mathbf{x},t)\equiv\frac{1}{2}[&(2\alpha-1)(1-P^{i,x}_\alpha)G^i_x(\mathbf{x},t)\\&+(2\beta-1)(1-P^{i,y}_\beta)G^i_y(\mathbf{x},t)\\&+(2\gamma-1)(1-P^{i,z}_\gamma)G^i_z(\mathbf{x},t)],\end{aligned} \tag{32}$$

where $G^i_\sigma(\mathbf{x},t)$ is a consequence of a finite-difference approximation (only requires a first-order accuracy) to the gradient along the σ Cartesian coordinate. Explicitly, these can be expressed as

$$\begin{aligned}G^i_\sigma(\mathbf{x},t)=&(1-w_\sigma)[N'_i(\mathbf{x}+\mathrm{sgn}(c_{i,x})\Delta_\sigma\hat{\boldsymbol{\sigma}},t)-N'_i(\mathbf{x},t)]\\&+w_\sigma[N'_i(\mathbf{x},t)-N'_i(\mathbf{x}-\mathrm{sgn}(c_{i,x})\Delta_\sigma\hat{\boldsymbol{\sigma}},t)].\end{aligned} \tag{33}$$

The choice of the parameter w_σ is rather arbitrary and corresponds to the chosen type of finite-difference for spatial derivatives. Specifically, a central difference is realized if $w_\sigma=1/2$, while an ''upper-wind'' scheme corresponds to $w_\sigma=1$. An analysis indicates that the greater value of w_σ leads to more positive hyperviscous effects and the system is always stable as long as $0\leqslant w_\sigma\leqslant 1$. To demonstrate such effects, a series of numerical simulations of transverse sinusoidal shear momentum decays was performed using the volumetrically formulated Boltzmann algorithm for the ratio $\Delta/c=8$. The corresponding measured viscosity values are presented in Fig. 1. The solid line represents the theoretical value of the regular viscosity associated with the underlying

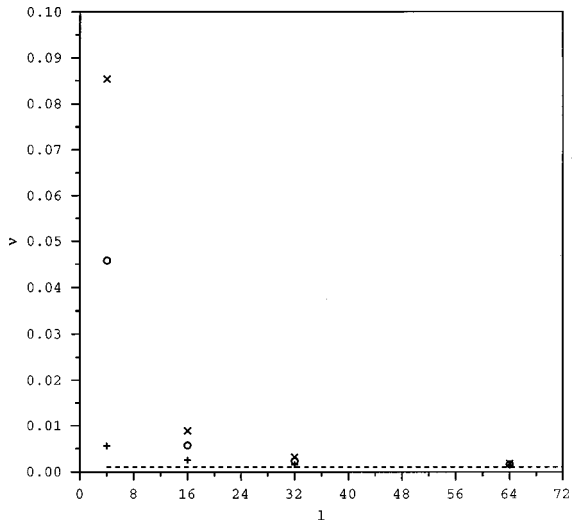

FIG. 1. Measured viscosity ν (in lattice units) as a function of wavelength l in cell unit. $T=0.42$ and $\tau=0.5025$. The solid line represents the theoretical value of the regular viscosity. The crosses, circles, and pluses are for $w_\sigma=0$, -0.04, and -0.08, respectively.

LB model. For the particular underlying BGK LB model used for these tests, its theoretical expression is given by

$$\nu=\left(\frac{\Delta t}{\tau}-\frac{1}{2}\right)T,$$

where T is the local temperature. From the measurement, we see that the volumetrically averaged Boltzmann system produces the same asymptotic viscosity value as that of the underlying fine grid LB at the long wavelength limit. However, the overall effective viscosity values form some cusplike shapes that peak at small wavelengths. This is an indication of an existence of hyperviscosity properties. Different choices of w_σ results in different hyperviscosity values. With a carefully chosen value of w_σ, such hyperviscous effects can be minimized without causing instability.

It can be directly verified algebraically that the state-flux function given above exactly satisfies the particle conservation condition

$$\sum_{\alpha=0}^{1}\sum_{\beta=0}^{1}\sum_{\gamma=0}^{1} F_i(\mathbf{x}\rightarrow\mathbf{x}+\mathbf{\Delta}^i_{\alpha\beta\gamma},t) = \sum_{\alpha=0}^{1}\sum_{\beta=0}^{1}\sum_{\gamma=0}^{1} P^{i,x}_\alpha P^{i,y}_\beta P^{i,z}_\gamma N'_i(\mathbf{x},t)=N'_i(\mathbf{x},t). \tag{34}$$

The additional contribution to fluxes $\delta N'_{i,\alpha\beta\gamma}(\mathbf{x},t)$ plays the role of redistributing particles among the fluxes but does not contribute any net change.

Several features of the present formulation can be compared to those of the pointwise interpolation scheme. First of all, because the summation upper bound is now 1 in Eq. (29) instead of 2 in Eq. (6), the number of neighboring points is significantly reduced (i.e., it is now 8 instead of 27). Though it requires an additional calculation of $G^i_\sigma(\mathbf{x},t)$ at each node, this also requires only nearest-neighbor information. Hence this algorithm is more local. Second, not only do they have simpler forms, but the weights defined in Eq. (31) are positive definite as opposed to those in Eq. (13). It has a form equivalent to a first-order pointwise interpolation. As a consequence, the positivity constraint for the distribution function can be explicitly enforced locally via the condition $N'_i(\mathbf{x},t)+\delta N'_{i,\alpha\beta\gamma}(\mathbf{x},t)\geqslant 0$. Because $N'_i(\mathbf{x},t)\geqslant 0$, the enforcement can be implemented easily by appropriately controlling the magnitude of $\delta N'_{i,\alpha\beta\gamma}(\mathbf{x},t)$ through reducing $G^i_\sigma(\mathbf{x},t)$ since the latter can be multiplied by any factor without compromising the conservation condition (34).

V. DISCUSSION

In this paper we have presented a volumetric formulation of the lattice Boltzmann dynamics. With properly chosen forms of the state-flux functions, both exact conservation laws and equilibrium balance conditions are achieved as in the original LBE. In addition, the positive-definite nature of the particle distribution functions can be explicitly enforced. The overall algorithm results in a self-consistent physical dynamical system, not merely a numerical method. Its macroscopic properties obey Navier-Stokes hydrodynamics up to the same viscous order of accuracy as the standard LBE on a finer lattice grid. The general formulation is applicable to an arbitrary mesh. As a reduced case on a uniform Cartesian mesh, the algorithm reduces to a significantly simple form and shows an advantage over those based on some second-order interpolation schemes. It can be viewed as a block spin realization of the underlying LBE on a lattice of finer resolution [18].

However, the present supergrid averaging approach does produce different (generally higher) hyperviscous effects compared to that of the original underlying LBE on a finer resolution lattice. This property has been verified numerically, demonstrating that the overall measured viscosity value increases as the flow length scale reduces. By trying various values of w_σ, without sacrificing stability, we can adjust or minimize such hyperviscous effects. An empirical optimal value to achieve a minimum hyperviscosity value is at $w_\sigma\sim -0.5c/\Delta_\sigma$, where c is the lattice unit of the original lattice. On the other hand, such a hyperviscosity effect is not entirely undesirable or unphysical. Borrowing the eddy viscosity concept [19], the unresolved spatial variations indeed tend to generate cusplike dissipations at short wavelengths close to the resolution boundary. Therefore, we do not need to necessarily eliminate it but to properly control its form and magnitude.

The volumetric approach is easily generalized to achieve a physical boundary conditions. For simplicity, we discuss the no-slip condition for the supergrid regular lattice case. The extension to the general mesh does not pose any fundamental differences. A no-slip condition for simple lattices can be realized at the kinetic level via the basic bounce-back process as defined by the simple relation

$$N'_i(\mathbf{x}-\hat{\mathbf{c}}_i,t)=N'_{i*}(\mathbf{x},t),$$

where $\mathbf{x}$ is a valid cell location adjacent to the boundary and $\mathbf{x}-\hat{\mathbf{c}}_i$ lies outside the fluid domain. $\hat{\mathbf{c}}_{i*}=-\hat{\mathbf{c}}_i$. The extension to the supergrid case is straightforward. For cell $\mathbf{x}$ adjacent to the boundary, the generalized bounce-back process is

to replace in Eq. (29) the state fluxes $F_i(\mathbf{x}-\boldsymbol{\Delta}^i_{\alpha\beta\gamma}\rightarrow\mathbf{x},t)$ associated with the nonexistent cells $\tilde{\mathbf{x}}=\mathbf{x}-\boldsymbol{\Delta}^i_{\alpha\beta\gamma}$ by $F_{i*}(\mathbf{x}\rightarrow\mathbf{x}+\boldsymbol{\Delta}^{i*}_{\alpha\beta\gamma},t)$ defined in Eq. (30). Obviously, $\mathbf{x}+\boldsymbol{\Delta}^{i*}_{\alpha\beta\gamma}=\mathbf{x}-\boldsymbol{\Delta}^i_{\alpha\beta\gamma}$. Without the additional terms $\delta N'_{i,\alpha\beta\gamma}(\mathbf{x},t)$, the above can be easily understood to be equivalent to the basic bounce-back process. On the other hand, there is an additional step in the extended bounce-back process for the supergrid case. That is, we need to properly construct the terms, $\delta N'_{i,\alpha\beta\gamma}(\mathbf{x},t)$ according to Eqs. (32) and (33). In fact, all we need to do is to replace either $N'_i(\mathbf{x}+\mathrm{sgn}(c_{i,x})\Delta_\sigma\hat{\boldsymbol{\sigma}},t)$ or $N'_i(\mathbf{x}-\mathrm{sgn}(c_{i,x})\Delta_\sigma\hat{\boldsymbol{\sigma}},t)$ by $N'_{i*}(\mathbf{x},t)$, depending upon whether $\mathbf{x}+\mathrm{sgn}(c_{i,x})\Delta_\sigma\hat{\boldsymbol{\sigma}}$ or $\mathbf{x}-\mathrm{sgn}(c_{i,x})\Delta_\sigma\hat{\boldsymbol{\sigma}}$ is a nonexistent cell site. It can be immediately verified that the overall bounce-back process described above for the supergrid lattice algorithm maintains mass and energy conservations in the system exactly. Because it involves fewer neighborhood sites and no negative propagations as opposed to the pointwise interpolation scheme [13], the current implementation of the no-slip boundary condition is more efficient and has a more clear physical meaning. Furthermore, in this volumatric representation, a no-slip surface is understood to be effectively located on the edges of these supergrid cells and the distances from the centers of these cells to the surface are naturally one-half of the cell unit (i.e., $\Delta/2$). As we know, this is necessary to produce a second-order accurate boundary condition [20].

Finally, we wish to suggest as a preliminary concept that the volumetric (block spin) constructions of the Boltzmann level representation may perhaps offer a possible alternative in formulating large eddy turbulence models. Instead of imposing an eddy viscosity form such as in the mixing-length approximation or deriving large-scale properties based on a Navier-Stokes level representation [19], we may systematically coarse grain the Boltzmann dynamics in which advection is essentially linear. The fundamental quantities that the volumetric scheme is calculating are the state-flux functions in the block averaged Boltzmann system. It is important to point out that the state-flux functions contain more information about the fluid properties within given scales than simply the fluid velocity field. Eddy-viscosity effects, and perhaps more, can be generated by such an alternative approach. Once formulated, we can use such a block averaged Boltzmann algorithm to perform large scale turbulent flow simulations. On the other hand, the resulting large-scale hydrodynamic equations may also be derived via a Chapman-Enskog transformation of such a Boltzmann system [21].

ACKNOWLEDGMENTS

The author wishes to thank Kim Molvig, James Hoch, and Chris Teixeira for their valuable discussions.

APPENDIX: PROOF OF THE THEOREM

According to Eqs. (22), (23), and (26) we have

$$F_i(\overline{\mathbf{x}}\rightarrow\overline{\mathbf{x}}',t)=\int_{D(\overline{\mathbf{x}})\cap D^{-i}(\overline{\mathbf{x}}')}\tilde{n}_i(\mathbf{x},t)d^3x+\theta_i(\overline{\mathbf{x}},t)\,\delta(\overline{\mathbf{x}}-\overline{\mathbf{x}}'),\tag{A1}$$

where

$$\tilde{n}_i(\mathbf{x},t)=n'_i(\overline{\mathbf{x}},t)+(\mathbf{x}-\overline{\mathbf{x}})\cdot\tilde{\boldsymbol{\nabla}}n'_i(\overline{\mathbf{x}},t)+\frac{1}{2}(\mathbf{x}-\overline{\mathbf{x}})(\mathbf{x}-\overline{\mathbf{x}}):\tilde{\boldsymbol{\nabla}}\tilde{\boldsymbol{\nabla}}n'_i(\overline{\mathbf{x}},t).\tag{A2}$$

The quantity $\delta(\overline{\mathbf{x}}-\overline{\mathbf{x}}')$ is a Kronecker delta function. The function $\theta_i(\overline{\mathbf{x}},t)$ is determined by the conservation condition

$$\sum_{\overline{\mathbf{x}}'}F_i(\overline{\mathbf{x}}\rightarrow\overline{\mathbf{x}}',t)=N'_i(\overline{\mathbf{x}},t)=V(\overline{\mathbf{x}})n'_i(\overline{\mathbf{x}},t).\tag{A3}$$

By directly substituting Eq. (A1) into the left-hand side of Eq. (A3) we get

$$\begin{aligned}\sum_{\overline{\mathbf{x}}'}F_i(\overline{\mathbf{x}}\rightarrow\overline{\mathbf{x}}',t)=\sum_{\overline{\mathbf{x}}'}\Bigg\{&\int_{D(\overline{\mathbf{x}})\cap D^{-i}(\overline{\mathbf{x}}')}n'_i(\overline{\mathbf{x}},t)d^3x\\&+\tilde{\boldsymbol{\nabla}}n'_i(\overline{\mathbf{x}},t)\cdot\int_{D(\overline{\mathbf{x}})\cap D^{-i}(\overline{\mathbf{x}}')}(\mathbf{x}-\overline{\mathbf{x}})d^3x\\&+\frac{1}{2}\tilde{\boldsymbol{\nabla}}\tilde{\boldsymbol{\nabla}}n'_i(\overline{\mathbf{x}},t):\int_{D(\overline{\mathbf{x}})\cap D^{-i}(\overline{\mathbf{x}}')}(\mathbf{x}-\overline{\mathbf{x}})\\&\times(\mathbf{x}-\overline{\mathbf{x}})d^3x\Bigg\}+\theta_i(\overline{\mathbf{x}},t).\end{aligned}\tag{A4}$$

Using the definition of $\overline{\mathbf{x}}$ as a geometric center defined by Eq. (15), the following essential properties are easily demonstrated:

$$\begin{aligned}&\sum_{\overline{\mathbf{x}}'}\int_{D(\overline{\mathbf{x}})\cap D^{-i}(\overline{\mathbf{x}}')}d^3x=\int_{D(\overline{\mathbf{x}})}d^3x=V(\overline{\mathbf{x}}),\\&\sum_{\overline{\mathbf{x}}'}\int_{D(\overline{\mathbf{x}})\cap D^{-i}(\overline{\mathbf{x}}')}(\mathbf{x}-\overline{\mathbf{x}})d^3x=\int_{D(\overline{\mathbf{x}})}(\mathbf{x}-\overline{\mathbf{x}})d^3x=0,\\&\sum_{\overline{\mathbf{x}}'}\int_{D(\overline{\mathbf{x}})\cap D^{-i}(\overline{\mathbf{x}}')}(\mathbf{x}-\overline{\mathbf{x}})(\mathbf{x}-\overline{\mathbf{x}})d^3x=\int_{D(\overline{\mathbf{x}})}(\mathbf{x}-\overline{\mathbf{x}})(\mathbf{x}-\overline{\mathbf{x}})d^3x.\end{aligned}\tag{A5}$$

We immediately see that Eq. (A4) becomes

$$\sum_{\overline{\mathbf{x}}'}F_i(\overline{\mathbf{x}}\rightarrow\overline{\mathbf{x}}',t)=V(\overline{\mathbf{x}})n'_i(\overline{\mathbf{x}},t)+\frac{1}{2}\tilde{\boldsymbol{\nabla}}\tilde{\boldsymbol{\nabla}}n'_i(\overline{\mathbf{x}},t):\int_{D(\overline{\mathbf{x}})}(\mathbf{x}-\overline{\mathbf{x}})(\mathbf{x}-\overline{\mathbf{x}})d^3x+\theta_i(\overline{\mathbf{x}},t).\tag{A6}$$

Thus

$$\theta_i(\overline{\mathbf{x}},t)=-\frac{1}{2}\tilde{\boldsymbol{\nabla}}\tilde{\boldsymbol{\nabla}}n'_i(\overline{\mathbf{x}},t):\int_{D(\overline{\mathbf{x}})}(\mathbf{x}-\overline{\mathbf{x}})(\mathbf{x}-\overline{\mathbf{x}})d^3x.\tag{A7}$$

With these expressions, the finite-volume LBE (17) becomes

$$N_i(\overline{\mathbf{x}},t+\Delta t)=\sum_{\overline{\mathbf{x}}'}\left\{n_i'(\overline{\mathbf{x}}',t)\int_{D(\overline{\mathbf{x}}')\cap D^{-i}(\overline{\mathbf{x}})}d^3x \quad +\boldsymbol{\nabla}n_i'(\overline{\mathbf{x}}',t)\cdot\int_{D(\overline{\mathbf{x}}')\cap D^{-i}(\overline{\mathbf{x}})}(\mathbf{x}-\overline{\mathbf{x}}')d^3x\right.$$
$$\left.+\frac{1}{2}\boldsymbol{\nabla}\boldsymbol{\nabla}n_i'(\overline{\mathbf{x}}',t):\int_{D(\overline{\mathbf{x}}')\cap D^{-i}(\overline{\mathbf{x}})}(\mathbf{x}-\overline{\mathbf{x}}')(\mathbf{x}-\overline{\mathbf{x}}')d^3x\right\} \quad +\theta_i(\overline{\mathbf{x}},t)+O(\boldsymbol{\nabla}^3). \tag{A8}$$

In the above, we have replaced $\tilde{\boldsymbol{\nabla}}$ by $\boldsymbol{\nabla}$, keeping in mind that their difference is $O(\boldsymbol{\nabla}^3)$ or higher. Taylor expanding Eq. (A8) up to $O(\boldsymbol{\nabla}^2)$ around $\overline{\mathbf{x}}$, we get

$$N_i(\overline{\mathbf{x}},t+\Delta t)=\sum_{\overline{\mathbf{x}}'}\left\{\left[n_i'(\overline{\mathbf{x}},t)+(\overline{\mathbf{x}}'-\overline{\mathbf{x}})\cdot\boldsymbol{\nabla}n_i'(\overline{\mathbf{x}},t)+\frac{1}{2}(\overline{\mathbf{x}}'-\overline{\mathbf{x}})(\overline{\mathbf{x}}'-\overline{\mathbf{x}}):\boldsymbol{\nabla}\boldsymbol{\nabla}n_i'(\overline{\mathbf{x}},t)\right]\right.$$
$$\times\int_{D(\overline{\mathbf{x}}')\cap D^{-i}(\overline{\mathbf{x}})}d^3x+[\boldsymbol{\nabla}n_i'(\overline{\mathbf{x}},t)+(\overline{\mathbf{x}}'-\overline{\mathbf{x}})\cdot\boldsymbol{\nabla}\boldsymbol{\nabla}n_i'(\overline{\mathbf{x}},t)]$$
$$\times\int_{D(\overline{\mathbf{x}}')\cap D^{-i}(\overline{\mathbf{x}})}(\mathbf{x}-\overline{\mathbf{x}}')d^3x$$
$$\left.+\frac{1}{2}\boldsymbol{\nabla}\boldsymbol{\nabla}n_i'(\overline{\mathbf{x}},t):\int_{D(\overline{\mathbf{x}}')\cap D^{-i}(\overline{\mathbf{x}})}(\mathbf{x}-\overline{\mathbf{x}}')(\mathbf{x}-\overline{\mathbf{x}}')d^3x\right\}+\theta_i(\overline{\mathbf{x}},t)+O(\boldsymbol{\nabla}^3). \tag{A9}$$

Lets examine the quantity

$$\sum_{\overline{\mathbf{x}}'}\int_{D(\overline{\mathbf{x}}')\cap D^{-i}(\overline{\mathbf{x}})}(\mathbf{x}-\overline{\mathbf{x}}')d^3x=\sum_{\overline{\mathbf{x}}'}\left[\int_{D(\overline{\mathbf{x}}')\cap D^{-i}(\overline{\mathbf{x}})}(\mathbf{x}-\overline{\mathbf{x}})d^3x-\int_{D(\overline{\mathbf{x}}')\cap D^{-i}(\overline{\mathbf{x}})}(\overline{\mathbf{x}}'-\overline{\mathbf{x}})d^3x\right]. \tag{A10}$$

However, it can be realized that by shifting the domain of integration we have

$$\sum_{\overline{\mathbf{x}}'}\int_{D(\overline{\mathbf{x}}')\cap D^{-i}(\overline{\mathbf{x}})}\mathbf{x}\,d^3x=\sum_{\overline{\mathbf{x}}'}\int_{D^i(\overline{\mathbf{x}}')\cap D(\overline{\mathbf{x}})}(\mathbf{x}-\hat{\mathbf{c}}_i)d^3x=\int_{D(\overline{\mathbf{x}})}(\mathbf{x}-\hat{c}_i)d^3x \tag{A11}$$

where $D^i(\overline{\mathbf{x}}')$ is the domain of $D(\overline{\mathbf{x}}')$ rigid-body translated by distance $\hat{c}_i$. Therefore, together with Eqs. (A5), Eq. (A10) becomes

$$\sum_{\overline{\mathbf{x}}'}\int_{D(\overline{\mathbf{x}}')\cap D^{-i}(\overline{\mathbf{x}})}(\mathbf{x}-\overline{\mathbf{x}}')d^3x=-\hat{\mathbf{c}}_iV(\overline{\mathbf{x}})-\sum_{\overline{\mathbf{x}}'}(\overline{\mathbf{x}}'-\overline{\mathbf{x}})\int_{D(\overline{\mathbf{x}}')\cap D^{-i}(\overline{\mathbf{x}})}d^3x. \tag{A12}$$

Inserting the result of Eq. (A12) into Eq. (A9), with the properties in Eq. (A5), we get

$$N_i(\overline{\mathbf{x}},t+\Delta t)=V(\overline{\mathbf{x}})[n_i'(\overline{\mathbf{x}},t)-\hat{\mathbf{c}}_i\cdot\boldsymbol{\nabla}n_i'(\overline{\mathbf{x}},t)]$$
$$+\sum_{\overline{\mathbf{x}}'}\left\{(\overline{\mathbf{x}}'-\overline{\mathbf{x}})\cdot\boldsymbol{\nabla}\boldsymbol{\nabla}n_i'(\overline{\mathbf{x}},t)\cdot\int_{D(\overline{\mathbf{x}}')\cap D^{-i}(\overline{\mathbf{x}})}(\mathbf{x}-\overline{\mathbf{x}})d^3x\right.$$
$$-\frac{1}{2}(\overline{\mathbf{x}}'-\overline{\mathbf{x}})(\overline{\mathbf{x}}'-\overline{\mathbf{x}}):\boldsymbol{\nabla}\boldsymbol{\nabla}n_i'(\overline{\mathbf{x}},t)\int_{D(\overline{\mathbf{x}}')\cap D^{-i}(\overline{\mathbf{x}})}d^3x$$
$$\left.+\frac{1}{2}\boldsymbol{\nabla}\boldsymbol{\nabla}n_i'(\overline{\mathbf{x}},t):\int_{D(\overline{\mathbf{x}}')\cap D^{-i}(\overline{\mathbf{x}})}(\mathbf{x}-\overline{\mathbf{x}}')(\mathbf{x}-\overline{\mathbf{x}}')d^3x\right\}+\theta_i(\overline{\mathbf{x}},t)+O(\boldsymbol{\nabla}^3). \tag{A13}$$

If we further write in the above

$$\int_{D(\overline{\mathbf{x}}')\cap D^{-i}(\overline{\mathbf{x}})}(\mathbf{x}-\overline{\mathbf{x}}')(\mathbf{x}-\overline{\mathbf{x}}')d^3x$$
$$=\int_{D(\overline{\mathbf{x}}')\cap D^{-i}(\overline{\mathbf{x}})}[(\mathbf{x}-\overline{\mathbf{x}})(\mathbf{x}-\overline{\mathbf{x}})$$
$$-(\mathbf{x}-\overline{\mathbf{x}})(\overline{\mathbf{x}}'-\overline{\mathbf{x}})-(\overline{\mathbf{x}}'-\overline{\mathbf{x}})(\mathbf{x}-\overline{\mathbf{x}})$$
$$+(\overline{\mathbf{x}}'-\overline{\mathbf{x}})(\overline{\mathbf{x}}'-\overline{\mathbf{x}})]d^3x, \tag{A14}$$

then Eq. (A13) is simplified to become

$$N_i(\overline{\mathbf{x}},t+\Delta t)$$
$$=V(\overline{\mathbf{x}})[n_i'(\overline{\mathbf{x}},t)-\hat{\mathbf{c}}_i\cdot\boldsymbol{\nabla}n_i'(\overline{\mathbf{x}},t)]$$
$$+\frac{1}{2}\boldsymbol{\nabla}\boldsymbol{\nabla}n_i'(\overline{\mathbf{x}},t):\sum_{\overline{\mathbf{x}}'}\int_{D(\overline{\mathbf{x}}')\cap D^{-i}(\overline{\mathbf{x}})}(\mathbf{x}-\overline{\mathbf{x}})(\mathbf{x}-\overline{\mathbf{x}})d^3x$$
$$+\theta_i(\overline{\mathbf{x}},t)+O(\boldsymbol{\nabla}^3). \tag{A15}$$

The second term on the right-hand side of the above equation can be further simplified,

$$\sum_{\overline{\mathbf{x}}'} \int_{D(\overline{\mathbf{x}}')\cap D^{-i}(\overline{\mathbf{x}})} (\mathbf{x}-\overline{\mathbf{x}})(\mathbf{x}-\overline{\mathbf{x}})d^3x$$

$$= \sum_{\overline{\mathbf{x}}'} \int_{D^i(\overline{\mathbf{x}}')\cap D(\overline{\mathbf{x}})} (\mathbf{x}-\overline{\mathbf{x}}-\hat{\mathbf{c}}_i)(\mathbf{x}-\overline{\mathbf{x}}-\hat{\mathbf{c}}_i)d^3x$$

$$= \int_{D(\overline{\mathbf{x}})} (\mathbf{x}-\overline{\mathbf{x}}-\hat{\mathbf{c}}_i)(\mathbf{x}-\overline{\mathbf{x}}-\hat{\mathbf{c}}_i)d^3x$$

$$= \int_{D(\overline{\mathbf{x}})} (\mathbf{x}-\overline{\mathbf{x}})(\mathbf{x}-\overline{\mathbf{x}})d^3x + V(\overline{\mathbf{x}})\hat{\mathbf{c}}_i\hat{\mathbf{c}}_i \qquad \text{(A16)}$$

so that we have

$$N_i(\overline{\mathbf{x}},t+\Delta t)$$
$$= V(\overline{\mathbf{x}})[n_i'(\overline{\mathbf{x}},t) - \hat{\mathbf{c}}_i\cdot\nabla n_i'(\overline{\mathbf{x}},t) + \tfrac{1}{2}\hat{\mathbf{c}}_i\hat{\mathbf{c}}_i:\nabla\nabla n_i'(\overline{\mathbf{x}},t)]$$
$$+ \frac{1}{2}\nabla\nabla n_i'(\overline{\mathbf{x}},t): \int_{D(\overline{\mathbf{x}})} (\mathbf{x}-\overline{\mathbf{x}})(\mathbf{x}-\overline{\mathbf{x}})d^3x$$
$$+ \theta_i(\overline{\mathbf{x}},t) + O(\nabla^3). \qquad \text{(A17)}$$

Comparing this result to Eq. (A7) for $\theta_i(\overline{\mathbf{x}},t)$, we finally arrive at the conclusion of Eq. (20), that is,

$$N_i(\overline{\mathbf{x}},t+\Delta t) = \sum_{\overline{\mathbf{x}}'} F_i(\overline{\mathbf{x}}'\rightarrow\overline{\mathbf{x}},t)$$
$$= V(\overline{\mathbf{x}})[n_i'(\overline{\mathbf{x}},t) - \hat{\mathbf{c}}_i\cdot\nabla n_i'(\overline{\mathbf{x}},t)$$
$$+ \tfrac{1}{2}\hat{\mathbf{c}}_i\hat{\mathbf{c}}_i:\nabla\nabla n_i'(\overline{\mathbf{x}},t)] + O(\nabla^3). \qquad \text{(A18)}$$

[1] U. Frisch, B. Hasslacher, and Y. Pomeau, Phys. Rev. Lett. **56**, 1505 (1986).

[2] U. Frisch, D. d'Humières, B. Hasslacher, P. Lallemand, Y. Pomeau, and J.-P. Rivet, Complex Syst. **1**, 649 (1987).

[3] S. Wolfram, J. Stat. Phys. **45**, 471 (1986).

[4] K. Molvig, P. Donis, J. Myczkowski, and G. Vichniac, in *Discrete Kinetic Theory, Lattice Gas Dynamics and Foundations of Hydrodynamics*, edited by R. Monaco (World Scientific, Singapore, 1988).

[5] Physica D **47** (1&2) (1991), special issue on lattice gas methods for PDE's: theory, application, and hardware, edited by G. D. Doolen.

[6] F. Higuera, S. Succi, and R. Benzi, Europhys. Lett. **9**, 345 (1989).

[7] S. Chen, H. Chen, D. Martinez, and W. Matthaeus, Phys. Rev. Lett. **67**, 3776 (1991); H. Chen, S. Chen, and W. Matthaeus, Phys. Rev. A **45**, 5339 (1992); Y. Qian, D. d'Humières, and P. Lallemand, Europhys. Lett. **17**, 479 (1992).

[8] H. Chen, C. Teixeira, and K. Molvig, Int. J. Mod. Phys. C **8**, 675 (1997).

[9] D. H. Rothman and J. M. Keller, J. Stat. Phys. **52**, 1119 (1988); A. K. Gunstensen, D. H. Rothman, S. Zaleski, and G. Zanetti, Phys. Rev. A **43**, 4320 (1991).

[10] H. Chen, S. Chen, G. Doolen, Y. C. Lee, and H. Rose, Phys. Rev. A **40**, 2850 (1989).

[11] X. Shan and H. Chen, Phys. Rev. E **47**, 1815 (1993); **49**, 2941 (1994).

[12] M. Swift, W. Osborn, and J. Yeomans, Phys. Rev. Lett. **75**, 830 (1995); M. Swift, S. Orlandini, W. Osborn, and J. Yeomans, Phys. Rev. E **54**, 5041 (1996).

[13] X. He, L. Luo, and M. Dembo, J. Comput. Phys. **129**, 357 (1996).

[14] R. Benzi, S. Succi, and M. Vergassola, Phys. Rep. **222**, 145 1992).

[15] B. Nadiga and D. Pullin, J. Comput. Phys. **112**, 162 (1994); B. Nadiga, J. Stat. Phys. **81**, 129 (1995); J. Comput. Phys. **121**, 271 (1995).

[16] P. Bhatnagar, E. Gross, and M. Krook, Phys. Rev. **94**, 511 (1954).

[17] N. Cao, S. Chen, S. Jin, and D. Martinez, Phys. Rev. E **55**, 21 (1997).

[18] N. Goldenfeld, *Lectures on Phase Transitions and the Renormalization Group* (Addison-Wesley, Reading, MA, 1992), L. Chen, N. Goldenfeld, and Y. Oono, Phys. Rev. E **54**, 376 (1996).

[19] V. Yakhot and S. Orszag, J. Sci. Comput. **1**, 2 (1986); Y. Zhou and G. Vahala, Phys. Rev. E **47**, 2503 (1993).

[20] S. Chen, D. Martinez, and R. Mei, Phys. Fluids **8**, 2527 (1996).

[21] C. Cercignani, *The Boltzmann Equation and Its Applications* (Springer-Verlag, Berlin, 1988).